The recognition and sensing of anions through 'positive allosteric effects' using simple urea-amide receptors

*Cidália M. G. dos Santos,[a] Thomas McCabe,[a] Graeme W. Watson,[b] Paul E. Kruger[a,c] and Thorfinnur Gunnlaugsson[a]**

Supporting Information

Index

1. Figures

Figure S1. ^{1}H NMR and ^{13}NMR of compound **1.**

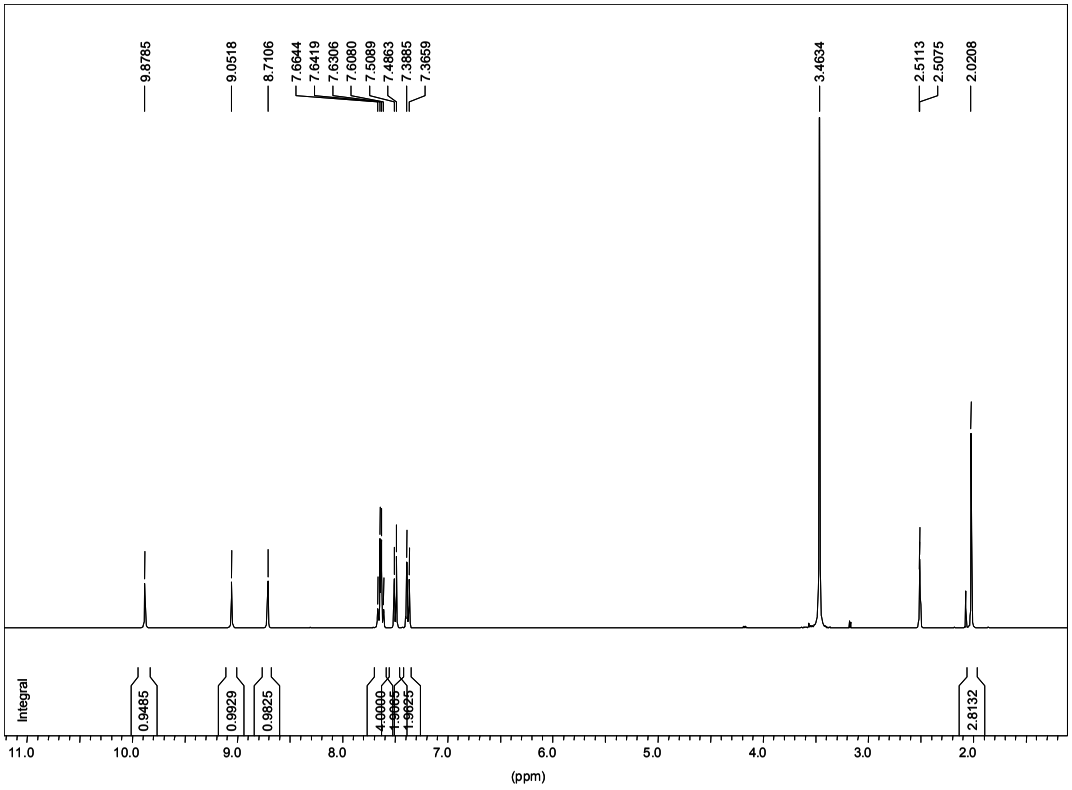

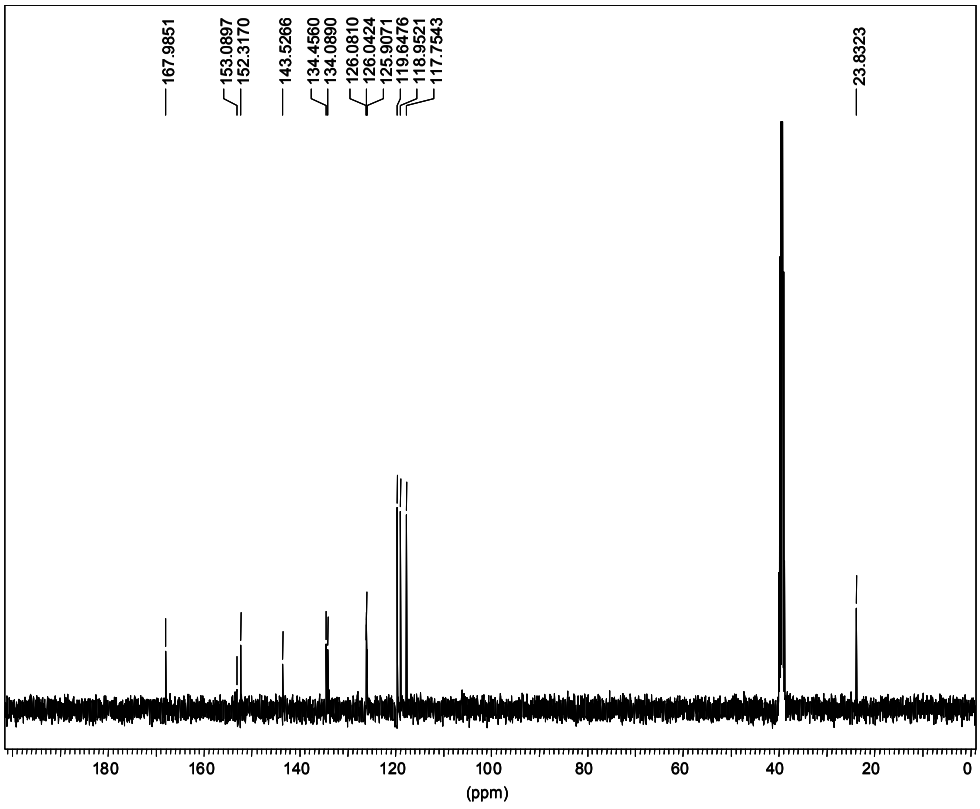

Figure S2. ^{1}H NMR and ^{13}NMR of compound **2.**

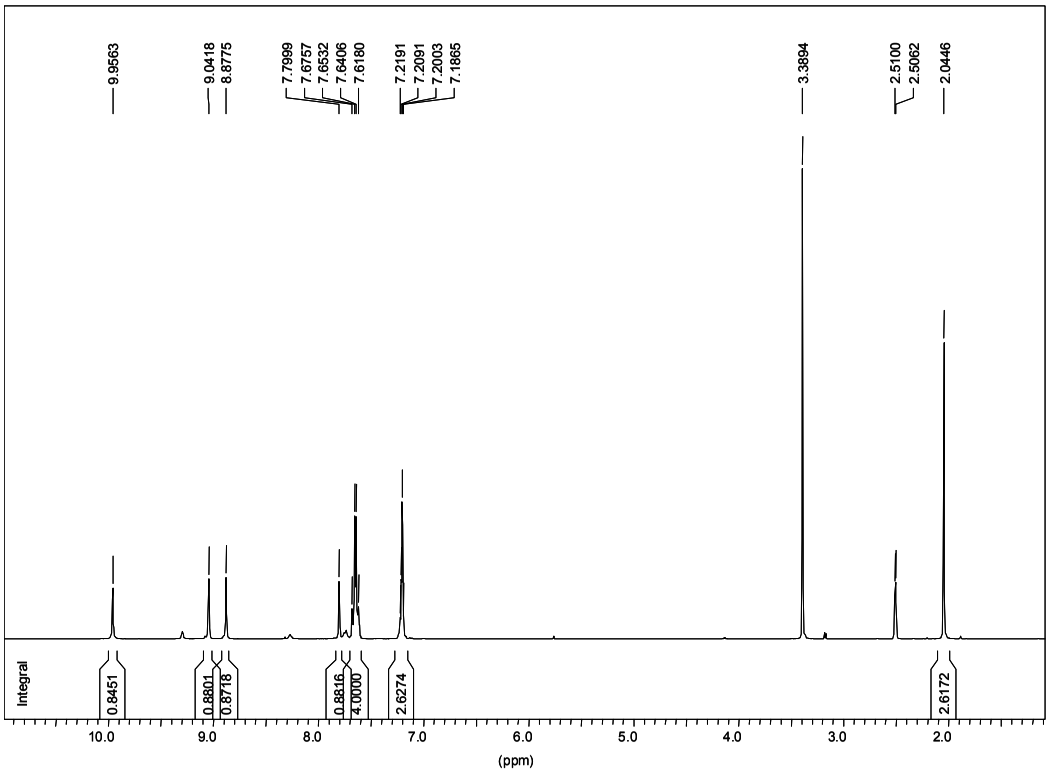

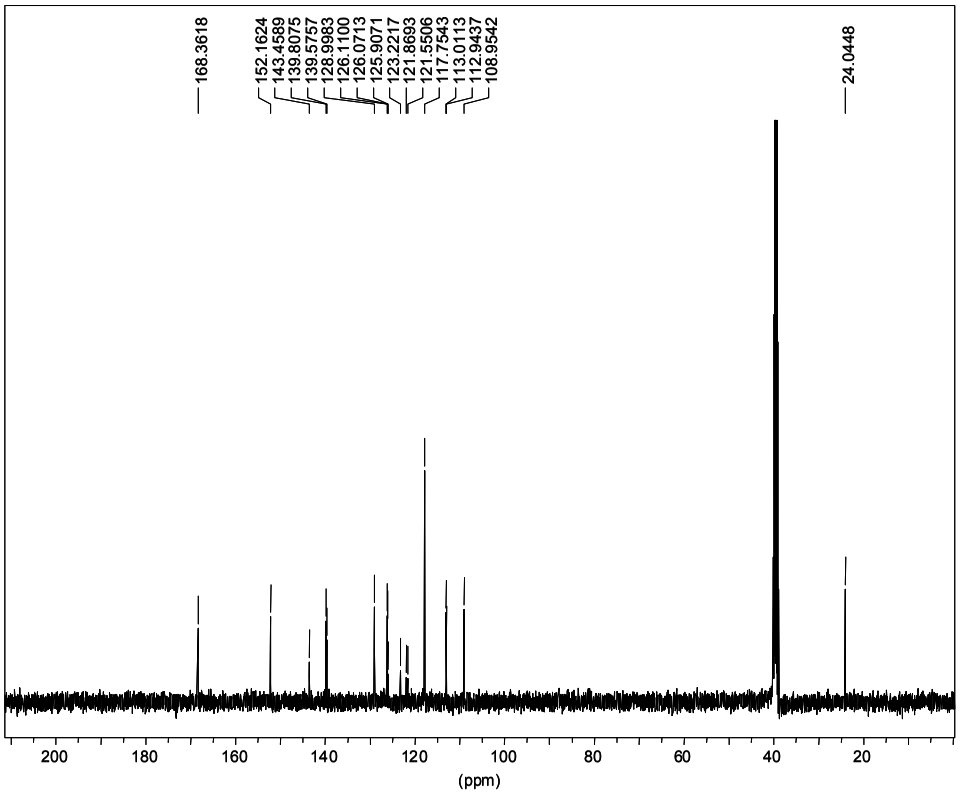

Figure S3. ^{1}H NMR and ^{13}NMR of compound **3.**

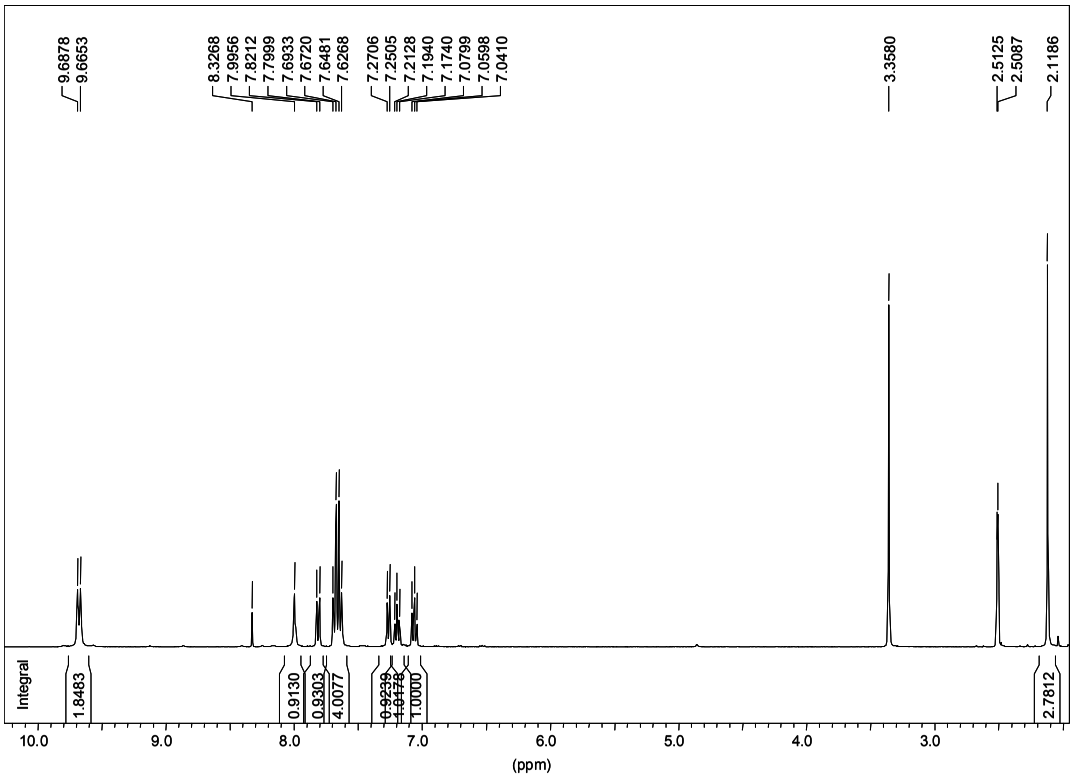

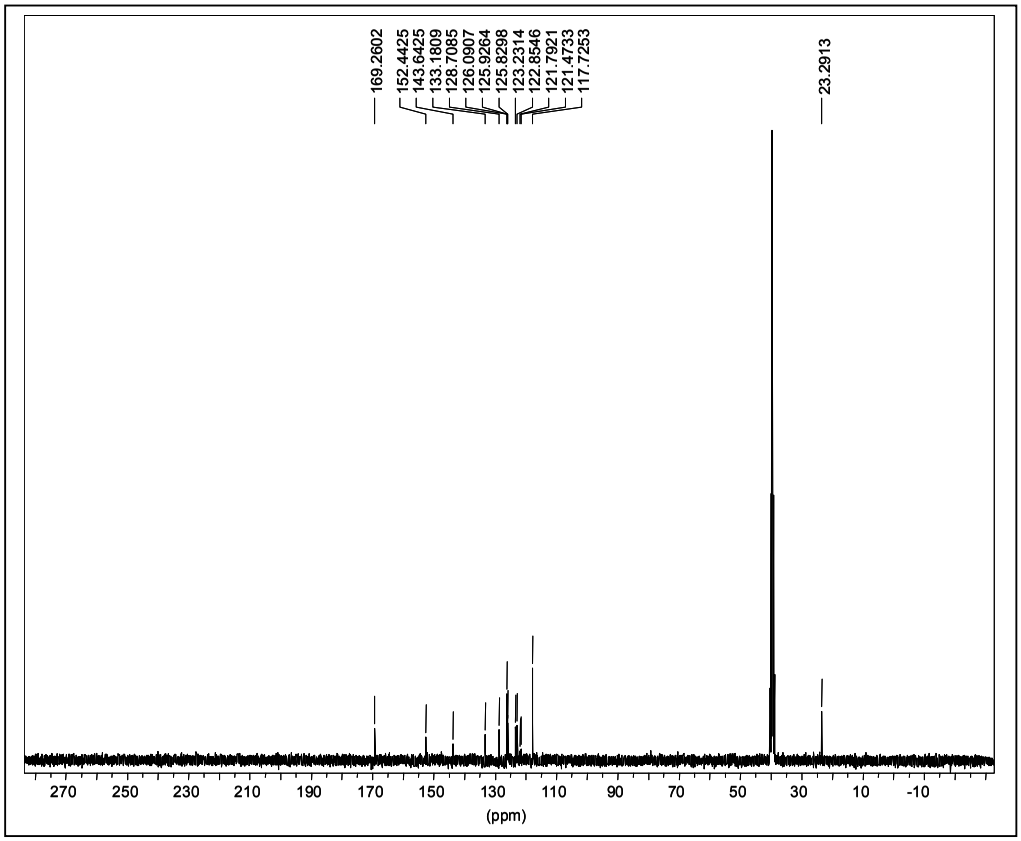

Figure S4. ^{19}F NMR of compounds **1-3.**

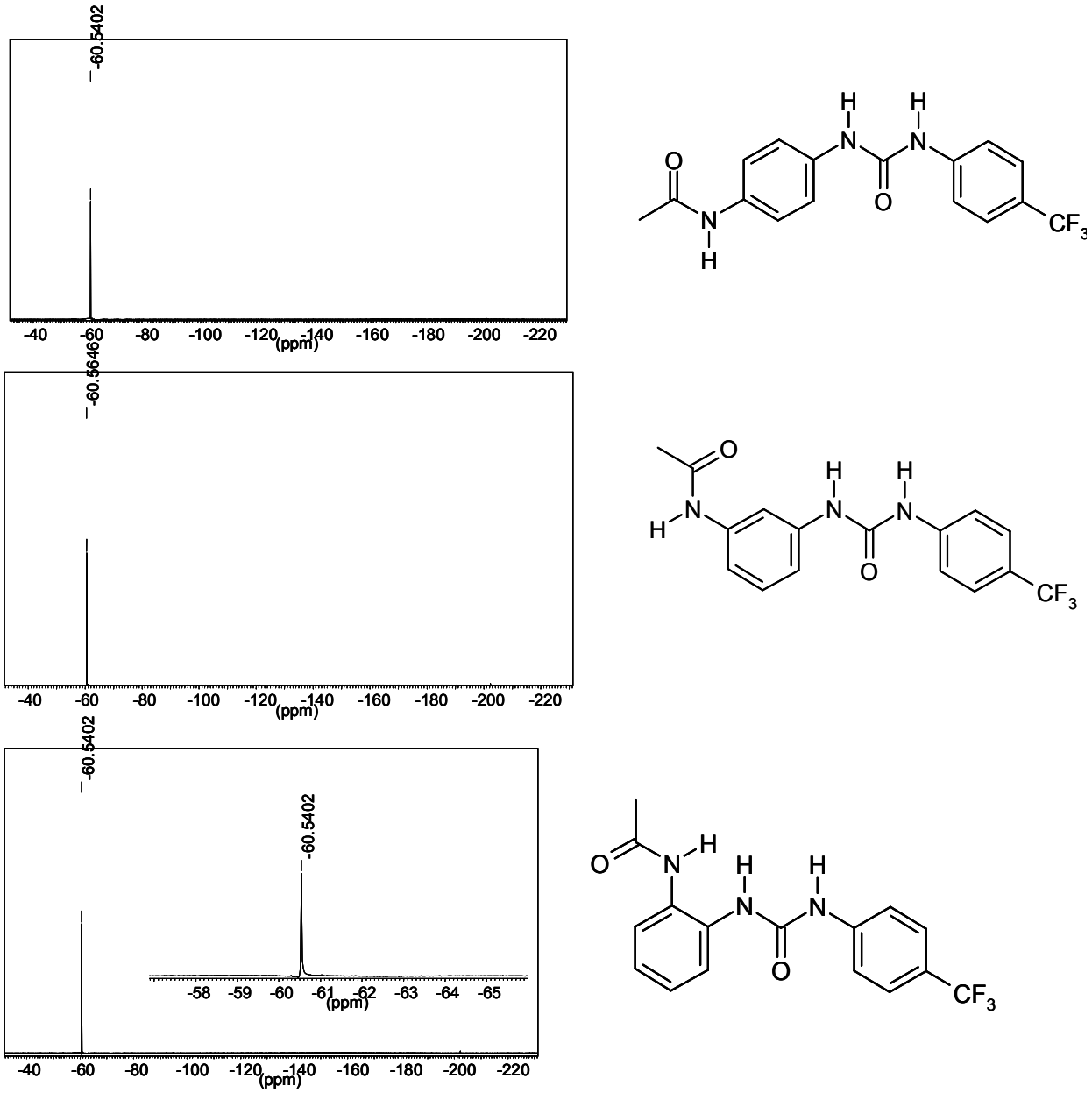

Figure S5. The packing diagram of **2** when viewed down the crystallographic *b-axis*.

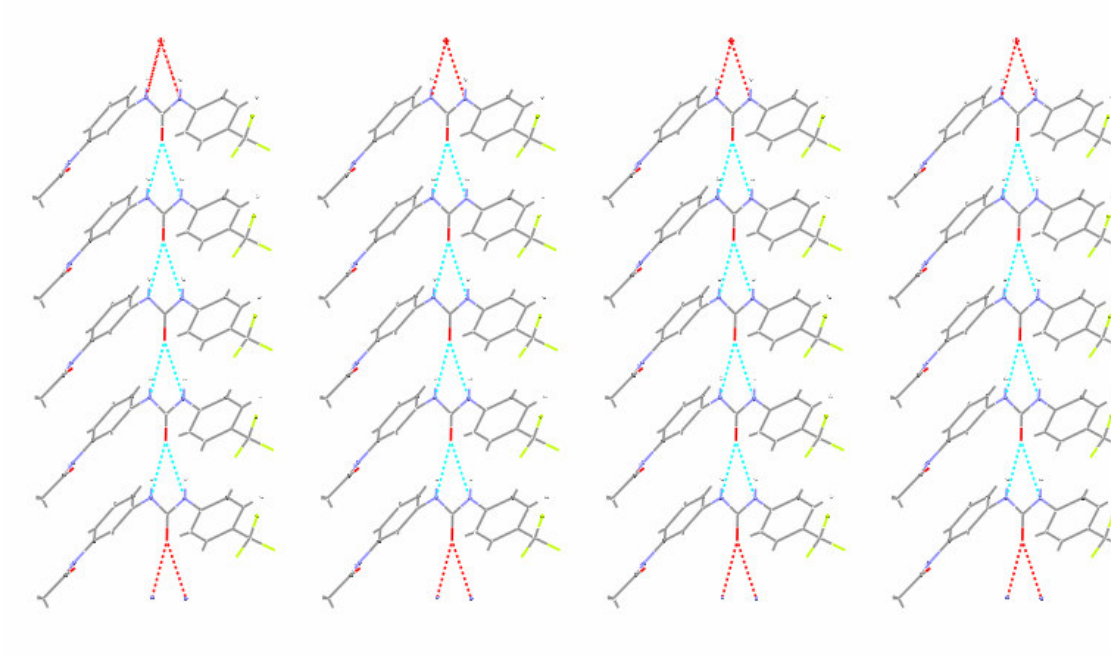

Figure S6. The packing diagram of **3** when viewed down the crystallographic *a-axis*.

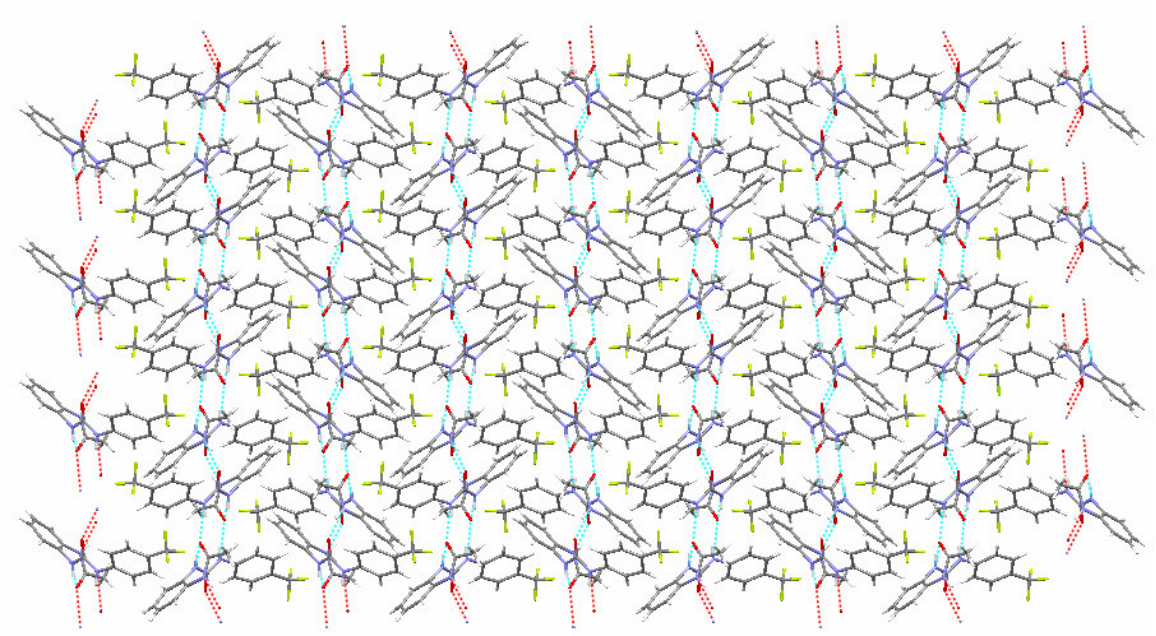

Figure S7. UV-Visible spectra showing the changes in the absorbance of **1** (4 μM) upon titration with $H_2P_2O_7^{2-}$ (0 – 1.72 mM) in MeCN.

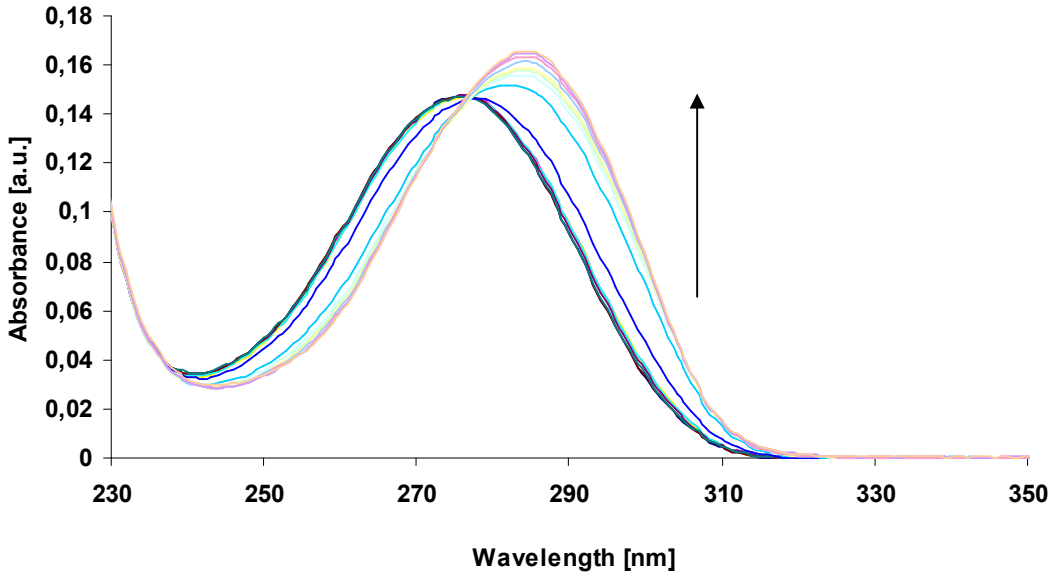

Figure S8. UV-Visible spectra showing the changes in the absorbance of **1** (4 μM) upon titration with AcO^- (0 – 1.48 mM) in MeCN.

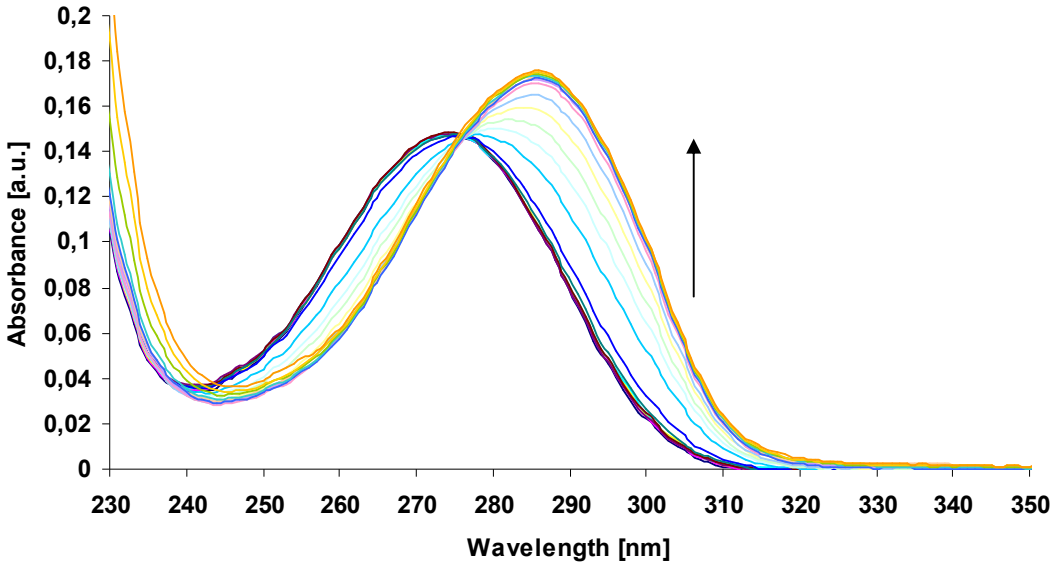

Figure S9. UV-Visible spectra showing the changes in the absorbance of **1** (4 μM) upon titration with F^- (0 – 1.65 mM) in MeCN.

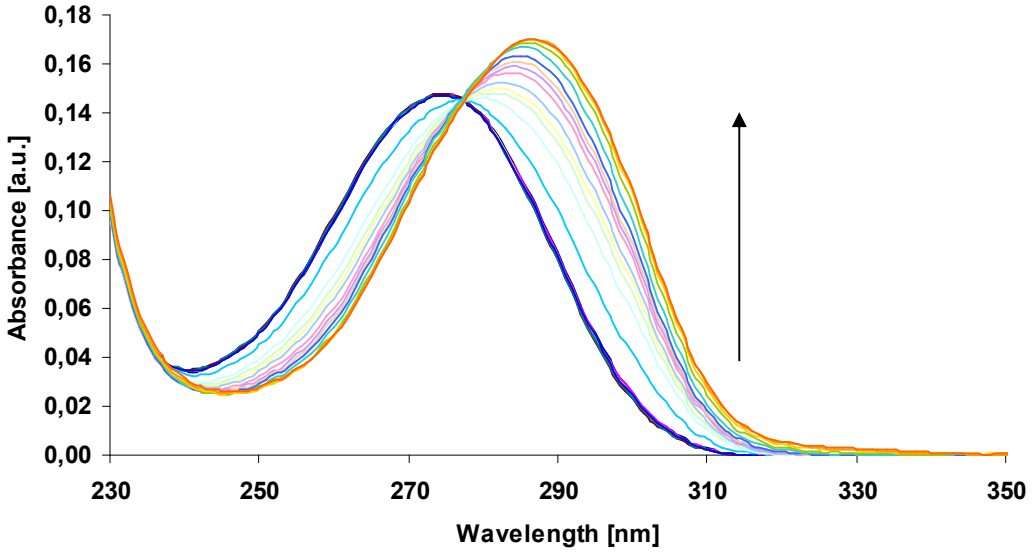

Figure S10. UV-Visible spectra showing the changes in the absorbance of **1** (4 μM) upon titration with Cl^- (0 – 2.38 mM) in MeCN.

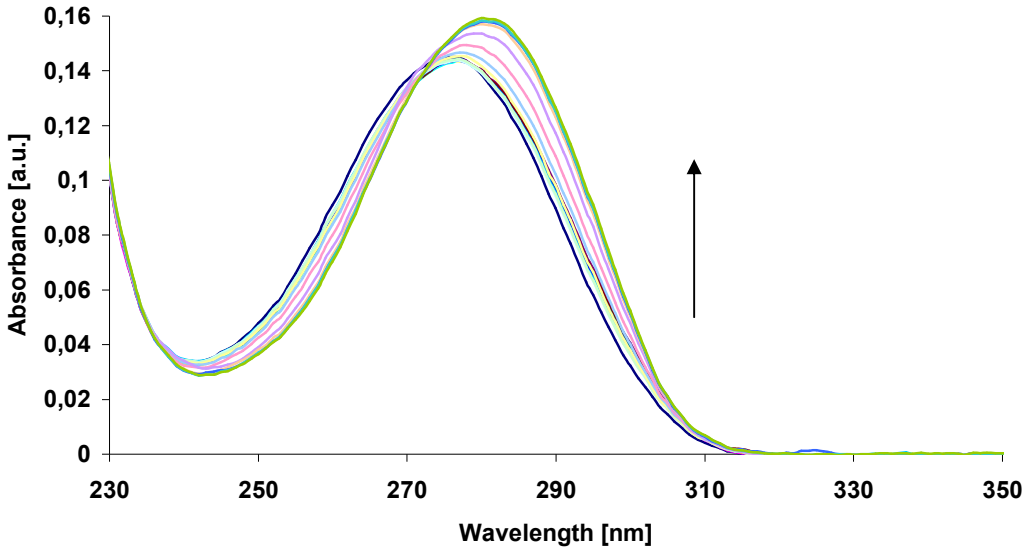

Figure S11. A) Experimental binding isotherm for the UV-Visible titration of **1** (4 μM) with AcO^- in MeCN and the corresponding fit obtained using SPECFIT. Data represented by the red circles, while the fit is represented by the solid black line. **B)** Corresponding speciation distribution diagram.

A)

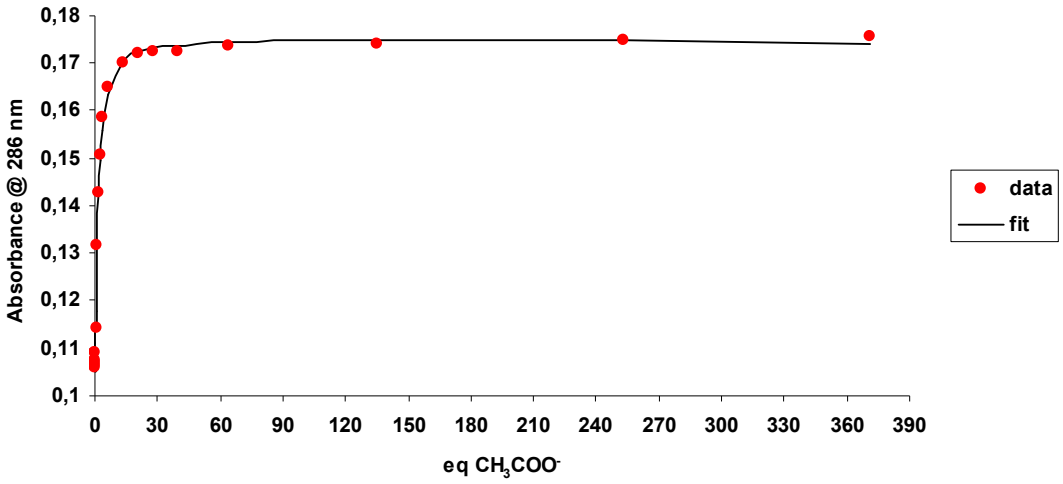

B)

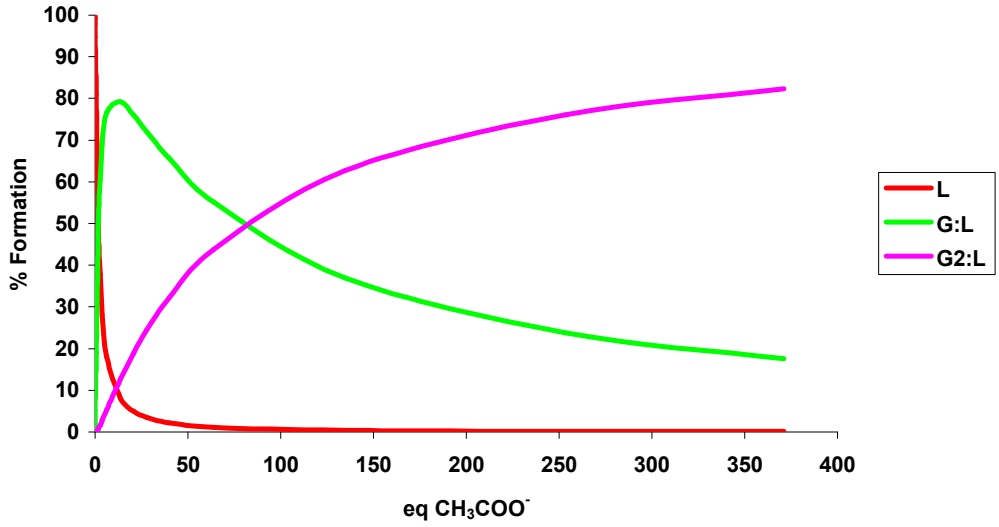

Figure S12. A) Experimental binding isotherm for the UV-Visible titration of **1** (4 μM) with F^- in MeCN and the corresponding fit obtained using SPECFIT. Data represented by the red circles, while the fit is represented by the solid black line. **B)** Corresponding speciation distribution diagram.

A)

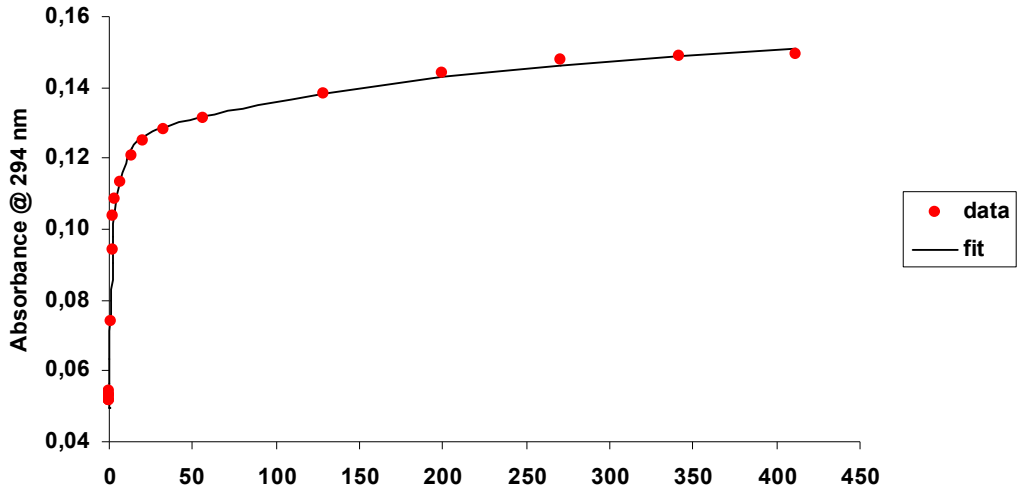

B)

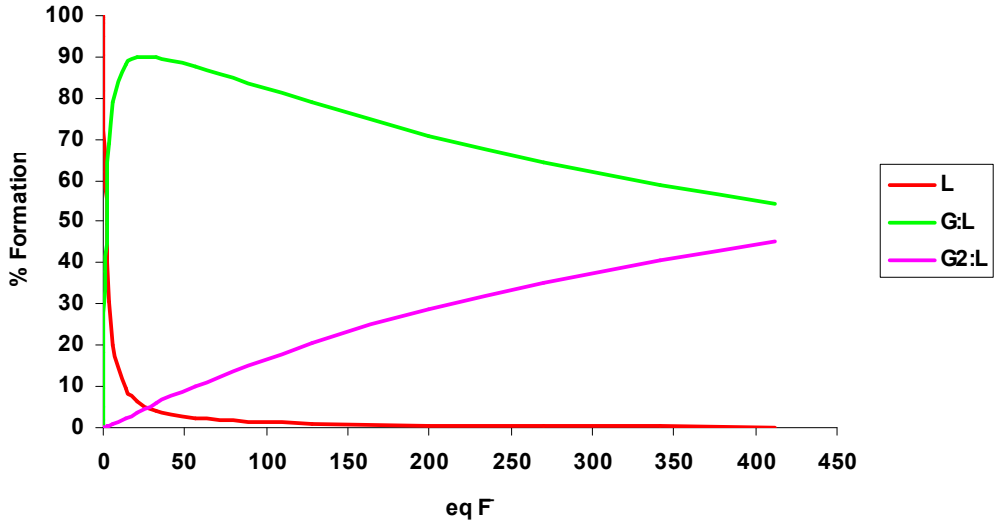

Figure S13. UV-Visible spectra showing the changes in the absorbance of **2** (4 μM) upon titration with $H_2PO_4^-$ (0 – 0.23 mM) in MeCN.

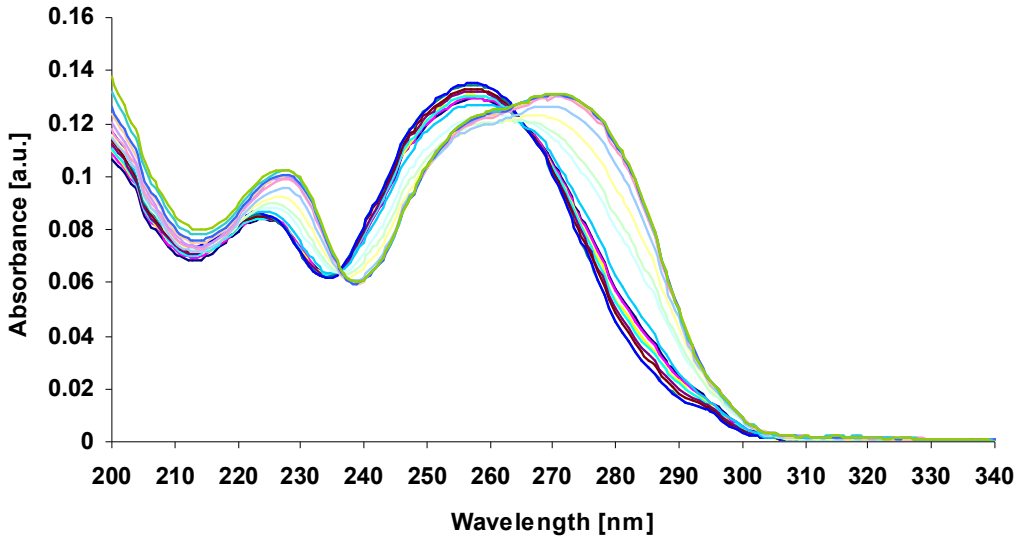

Figure S14. A) UV-Visible spectra showing the changes in the absorbance of **2** (4 μM) upon titration with F^- (0 – 0.24 mM) in MeCN. B) Corresponding speciation distribution diagram.

A)

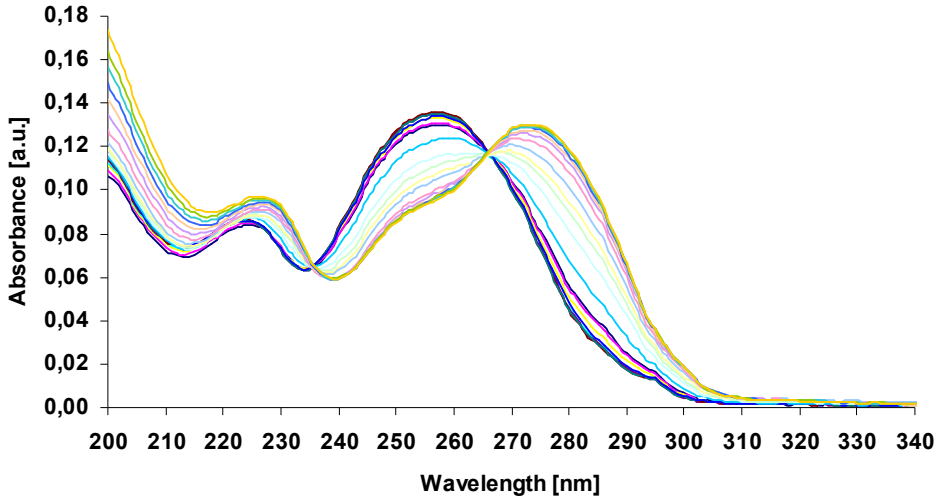

B)

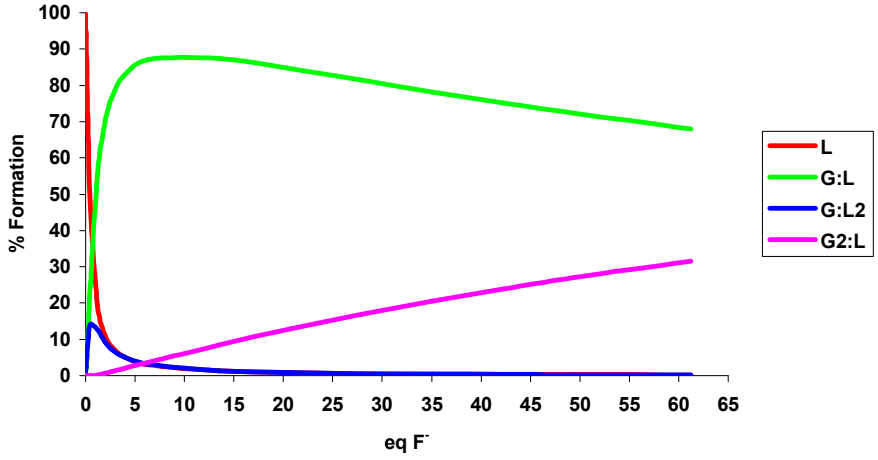

Figure S15. A) UV-Visible spectra showing the changes in the absorbance of **2** (4 μM) upon titration with $H_2P_2O_7^{2-}$ (0 – 0.92 mM) in MeCN. B) Corresponding speciation distribution diagram.

A)

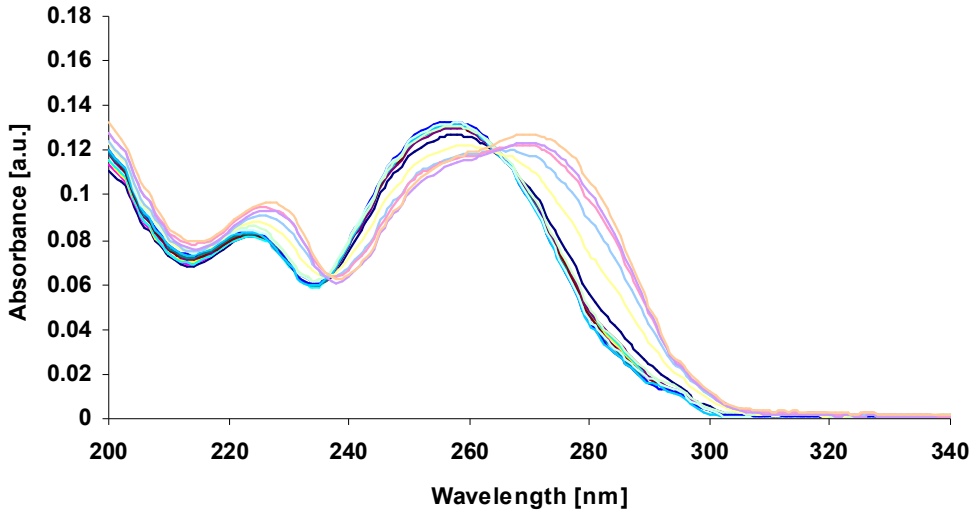

B)

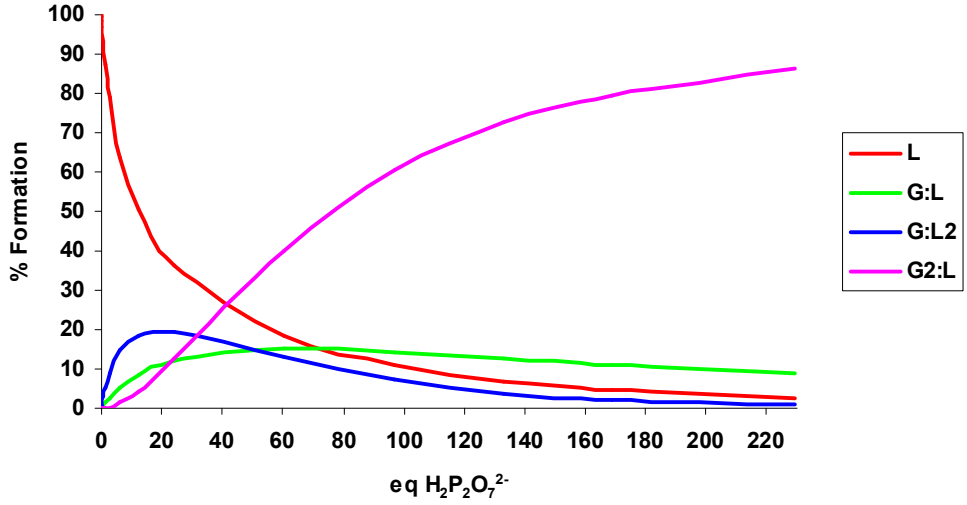

Figure S16. A) UV-Visible spectra showing the changes in the absorbance of **2** (4 μM) upon titration with Cl^- (0 – 2,38 mM) in MeCN. B) Corresponding speciation distribution diagram.

A)

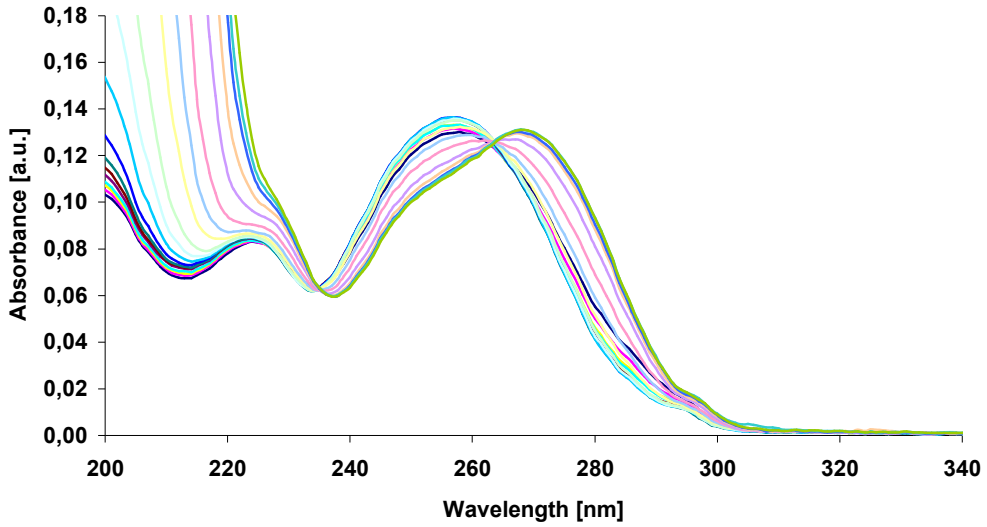

B)

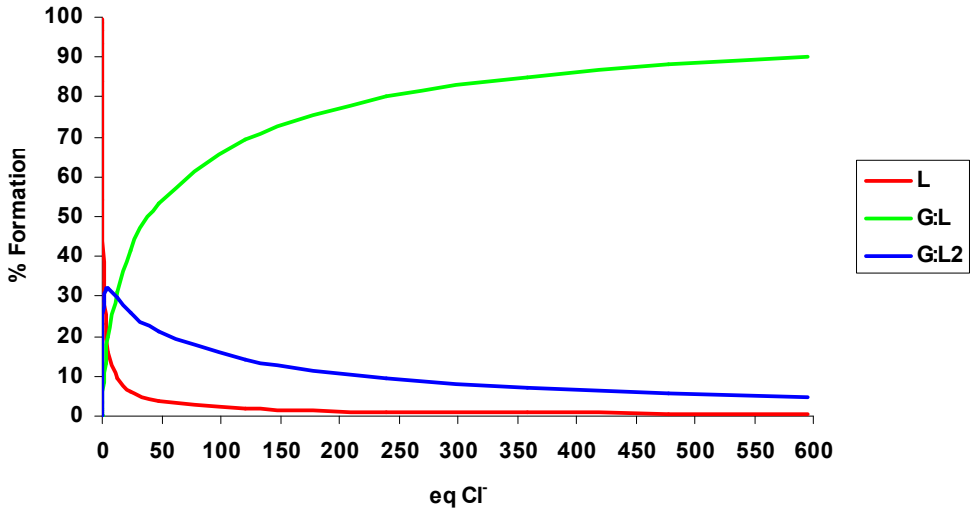

Figure S17. A) UV-Visible spectra showing the changes in the absorbance of **3** (4 μM) upon titration with $H_2PO_4^-$ $^-$ (0 – 40 μM) in MeCN. B) Corresponding speciation distribution diagram.

A)

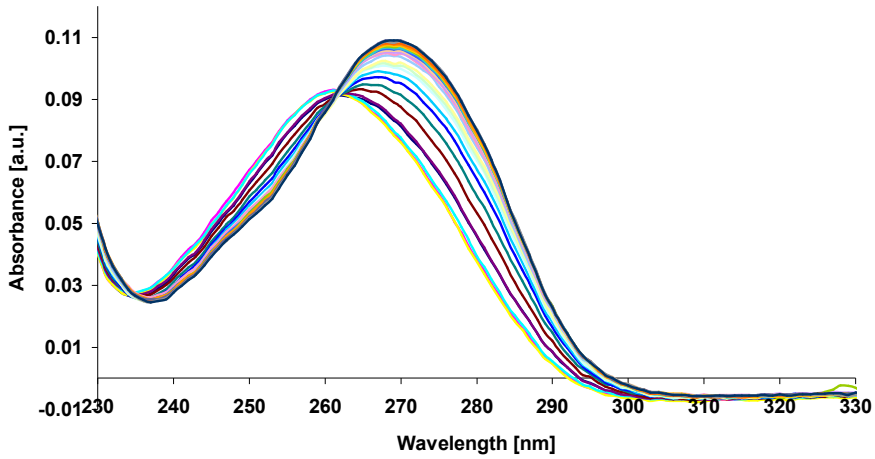

B)

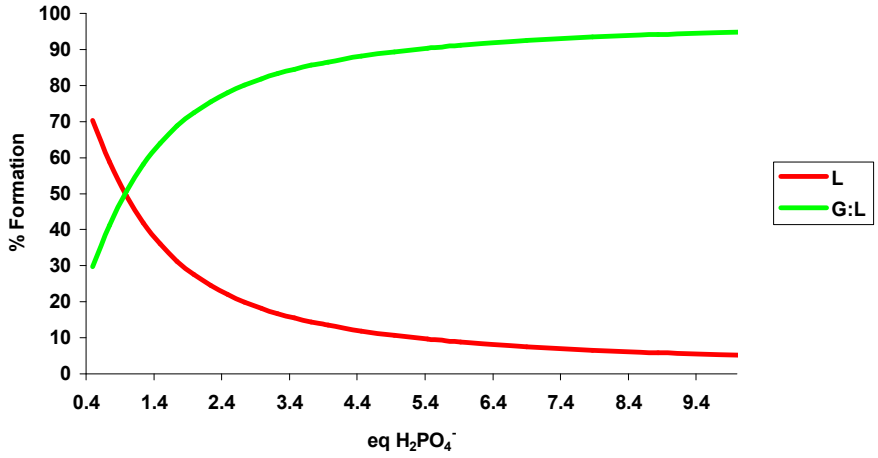

Figure S18. A) UV-Visible spectra showing the changes in the absorbance of **3** (4 μM) upon titration with $H_2P_2O_7^{2-}$ (0 – 40.1 μM) in MeCN. B) Corresponding speciation distribution diagram.

A)

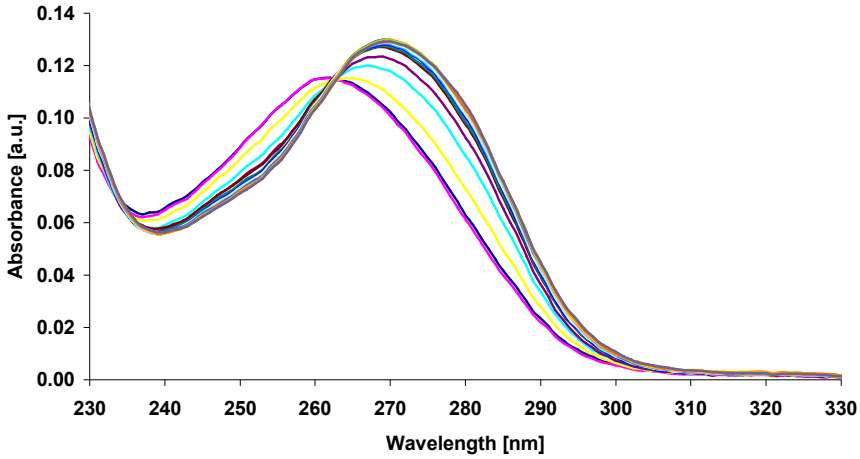

B)

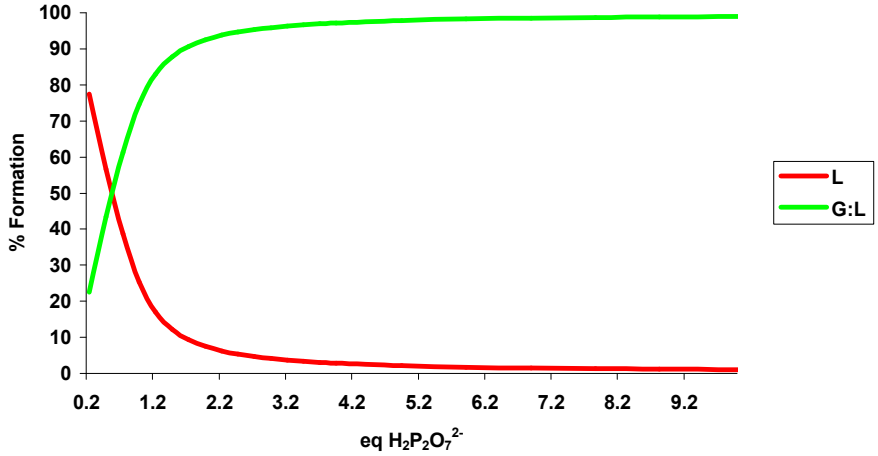

Figure S19. A) UV-Visible spectra showing the changes in the absorbance of **3** (4 μM) upon titration with F^- (0 – 40.1 μM) in MeCN. B) Corresponding speciation distribution diagram.

A)

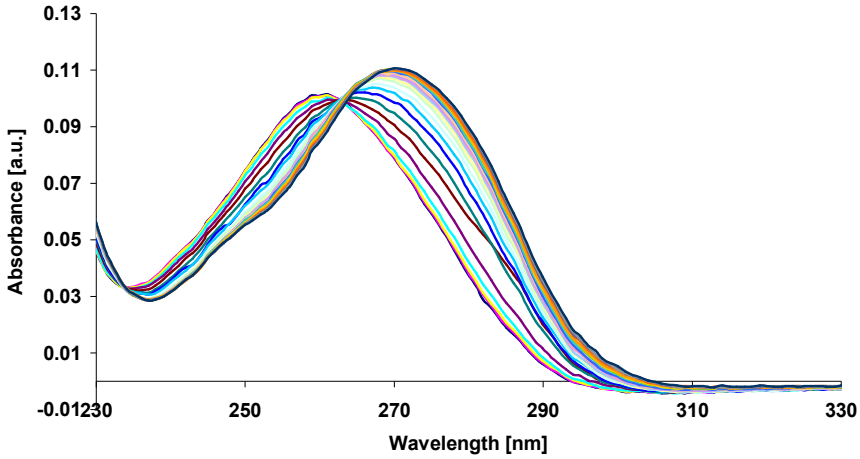

B)

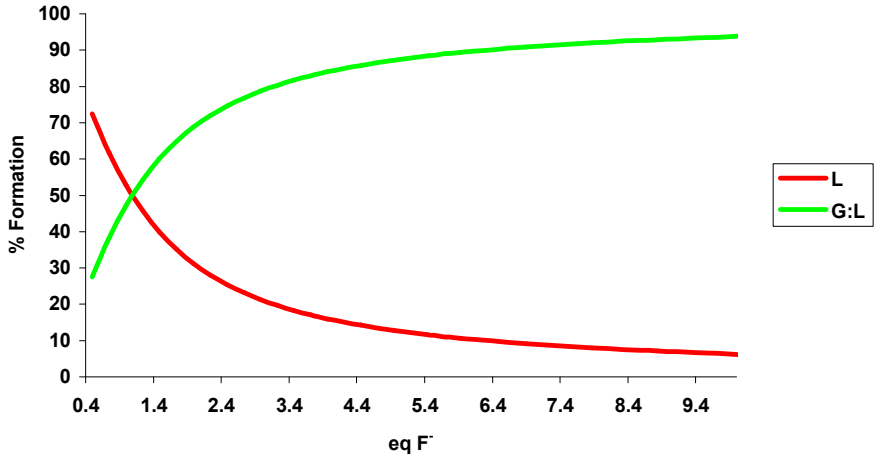

Figure S20. A) UV-Visible spectra showing the changes in the absorbance of **3** (4 μM) upon titration with Cl^- (0 – 40.1 μM) in MeCN. B) Corresponding speciation distribution diagram.

A)

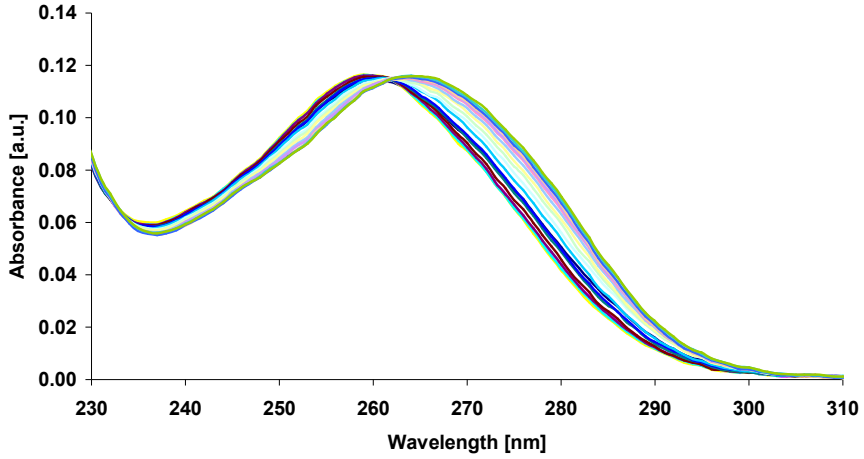

B)

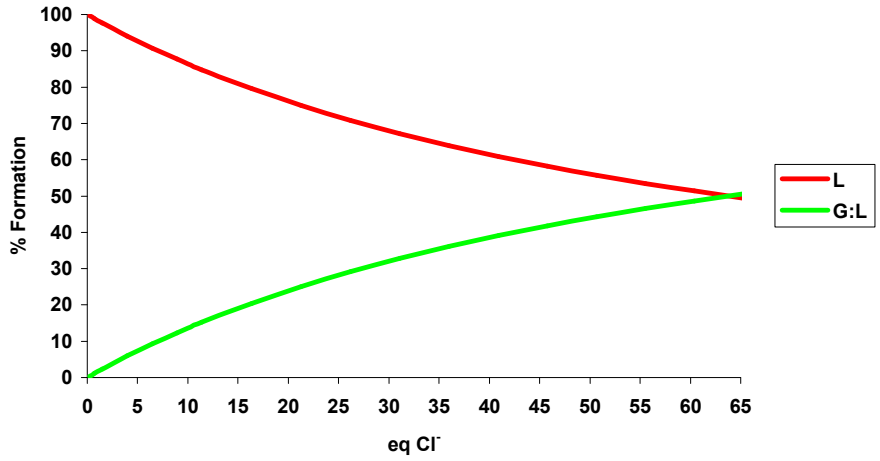

Figure S21. The stack plot of the ^{1}H-NMR (400 MHz, DMSO-d_6) spectra of **1** upon addition of 0, 0.6, 1 and 3 equivalents of AcO^{-}. H1-H3 are the N-H protons (NH1-NH3 in text).

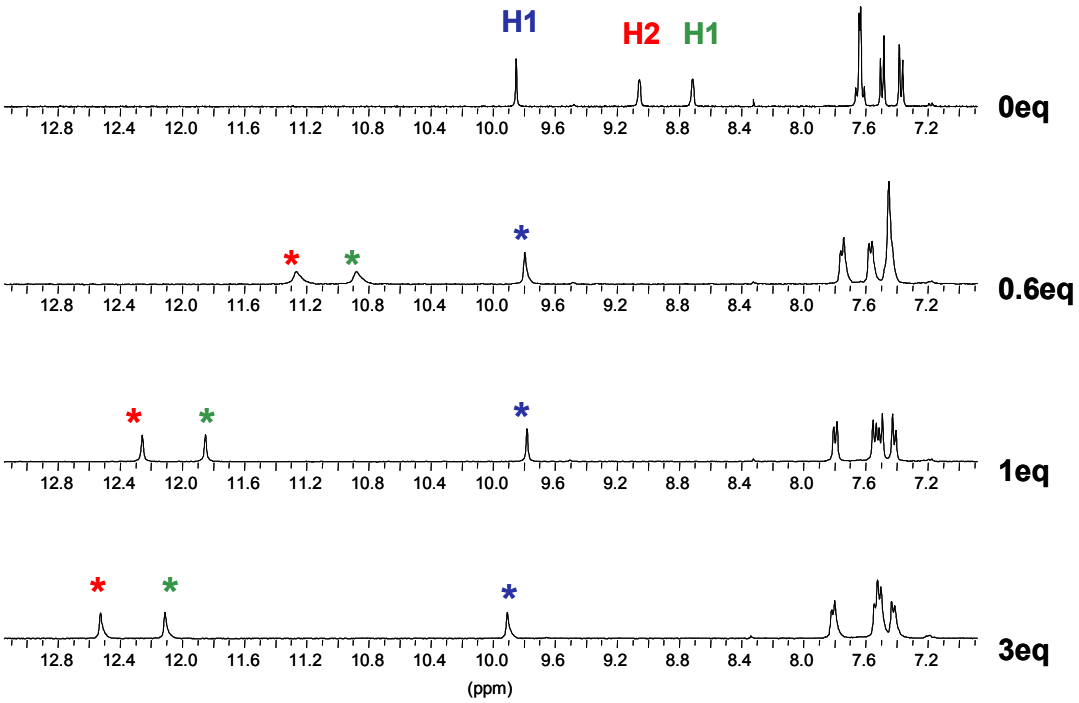

Figure S22. The stack plot of the ^{1}H-NMR (400 MHz, DMSO-d_6) spectra of **3** upon addition of 0, 0.5, 1 and 3 equivalents of AcO^{-}. H1-H3 are the N-H protons (NH1-NH3 in text).

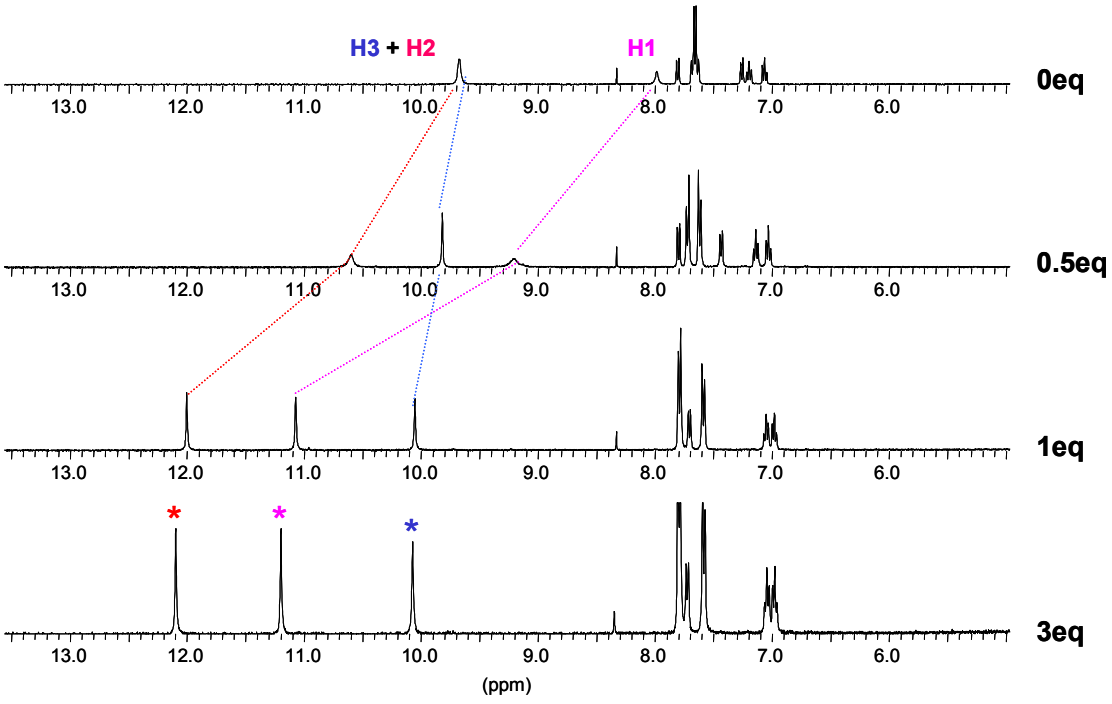

Figure S23. a) Changes in the NH1 and NH2 resonance of **1** (as Δδ) upon titration with AcO^-. b) The changes seen for the NH3 resonance during the same titration.

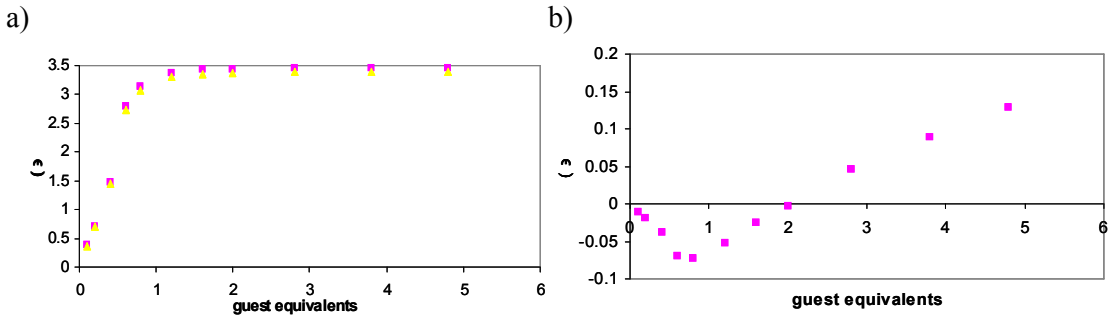

Figure S24. The stack plot of the ^{1}H-NMR (400 MHz, DMSO-d_6) spectra of **1** upon addition of 0, 0.6, 1 and 3 equivalents of $H_2PO_4^-$. H1-H3 are the N-H protons (NH1-NH3 in text).

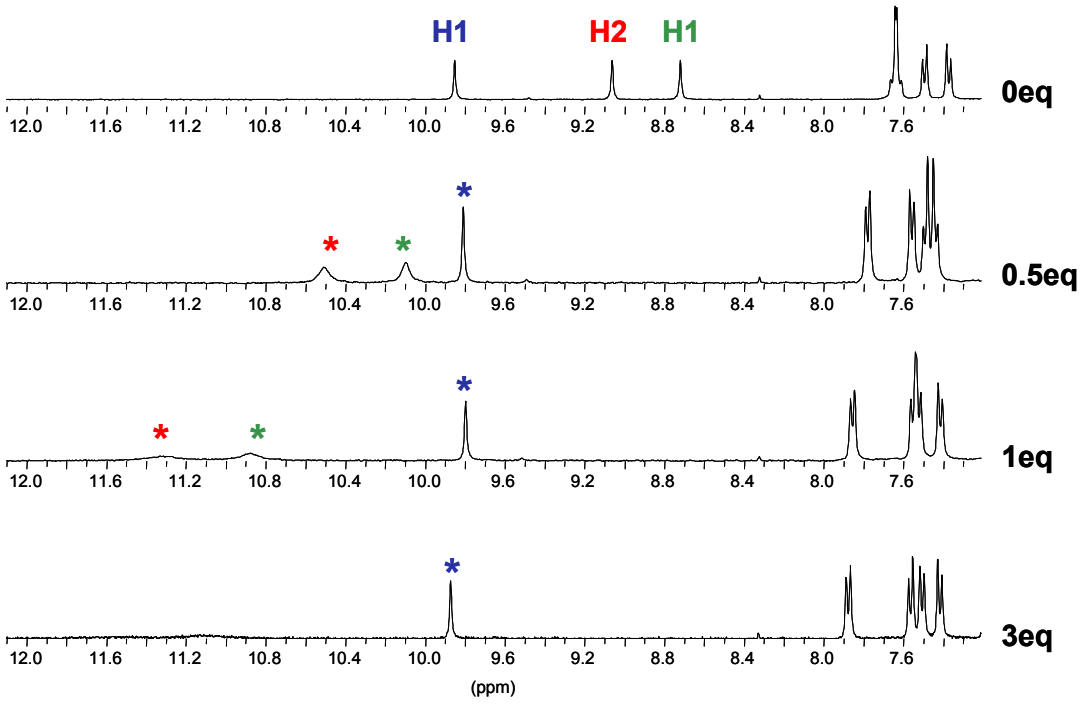

Figure S25. The stack plot of the ^{1}H-NMR (400 MHz, DMSO-d_6) spectra of **2** upon addition of 0, 1, 2.2 and 3 equivalents of $H_2PO_4^-$. H1-H3 are the N-H protons (NH1-NH3 in text).

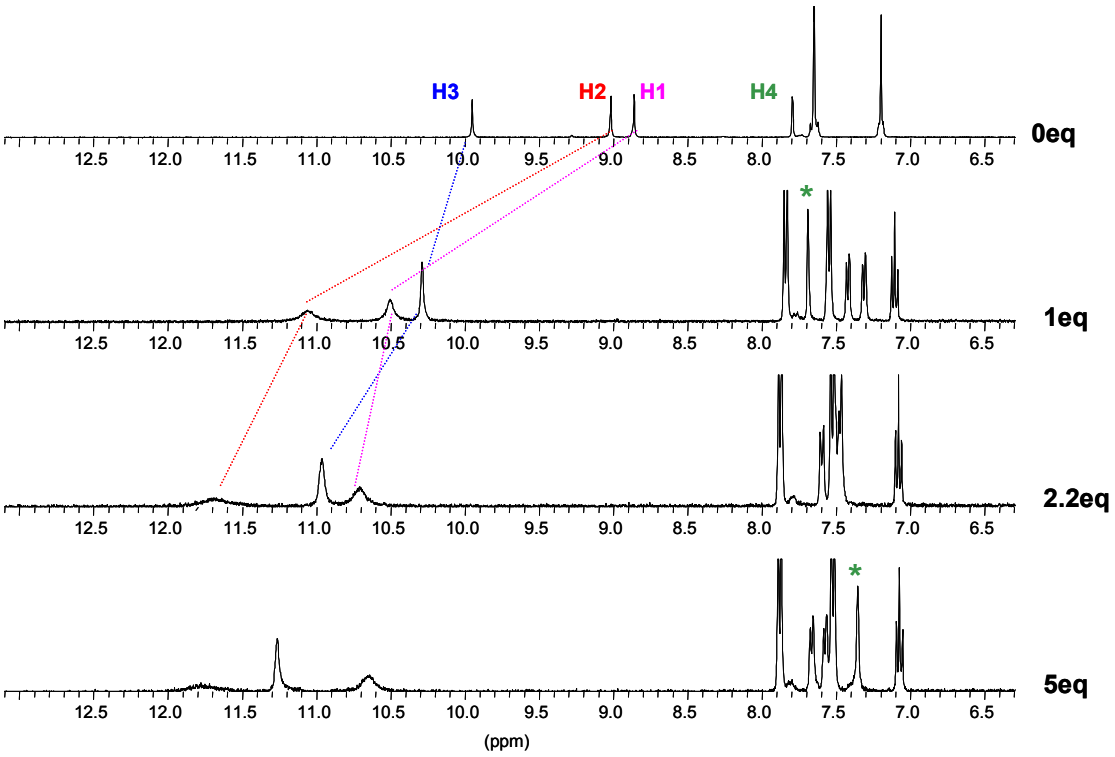

Figure S26. a) Changes in the NH1 and NH2 resonance of **3** (as Δδ) upon titration with $H_2PO_4^-$. b) The changes seen for the NH3 resonance during the same titration.

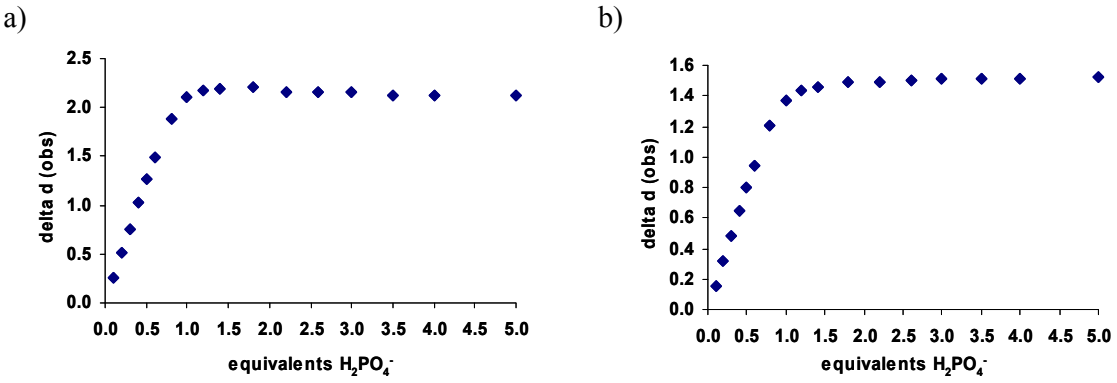

Figure S27. The stack plot of the ^{1}H-NMR (400 MHz, DMSO-d_6) spectra of **3** upon addition of 0, 1, 2.2 and 3 equivalents of Cl^-. H1-H3 are the N-H protons (NH1-NH3 in text).

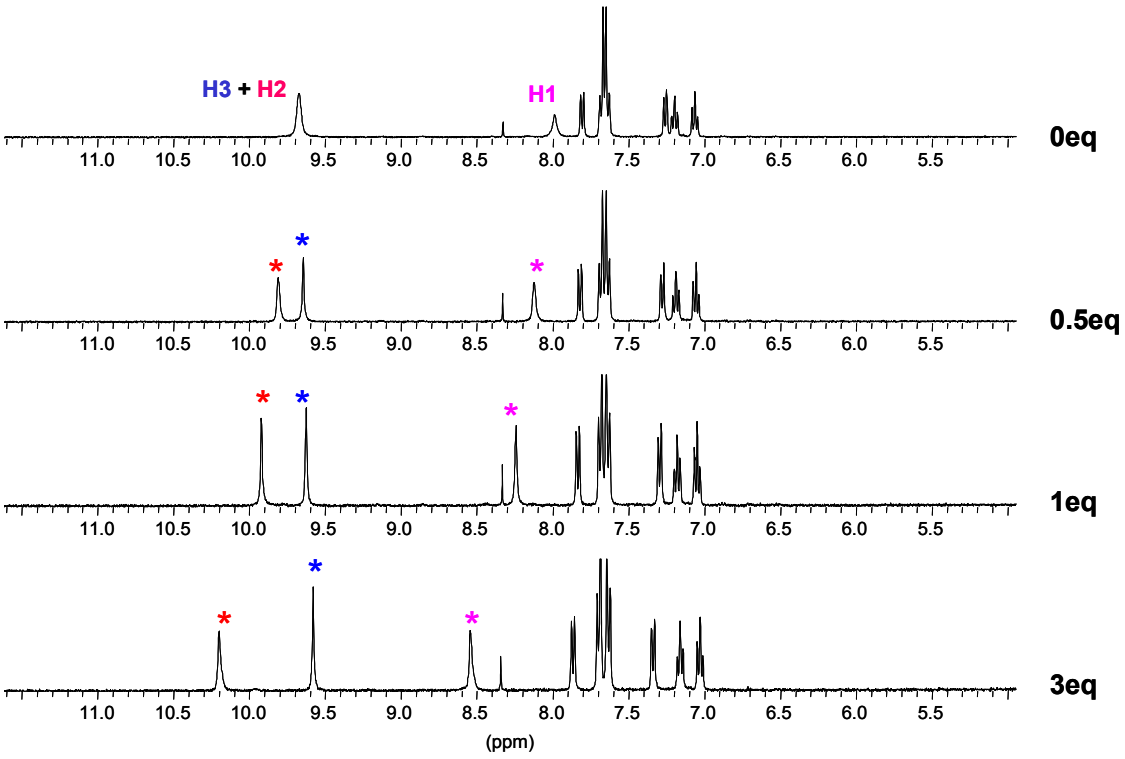

Figure S28. a) Changes in the NH2 resonance of **3** (as Δδ) upon titration with Cl^-.

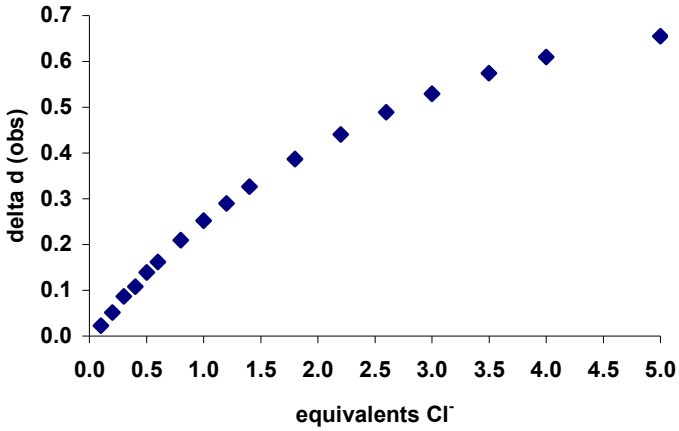

Figure S29. X-ray crystal structure of compound **1** with ellipsoids drawn at the 50% probability level.

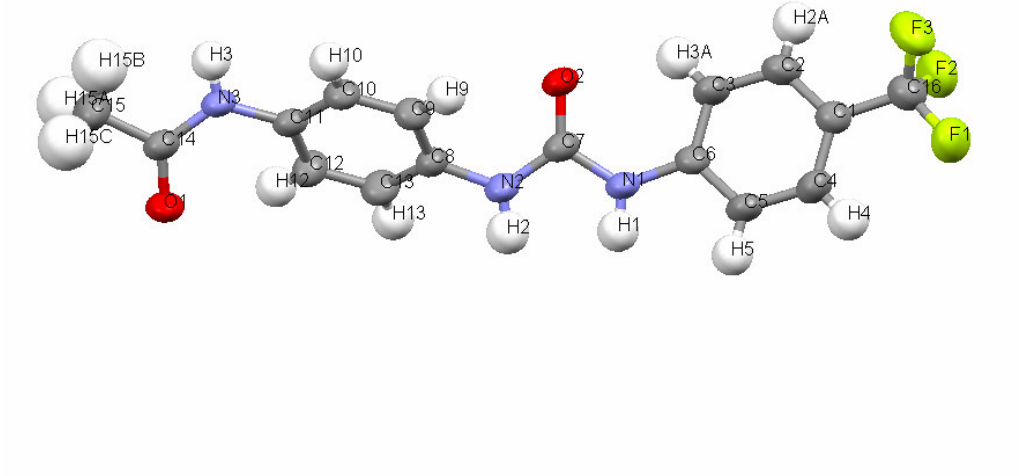

Figure S30. X-ray crystal structure of compound **2** with ellipsoids drawn at the 50% probability level. Solvent methanol has been removed for clarity.

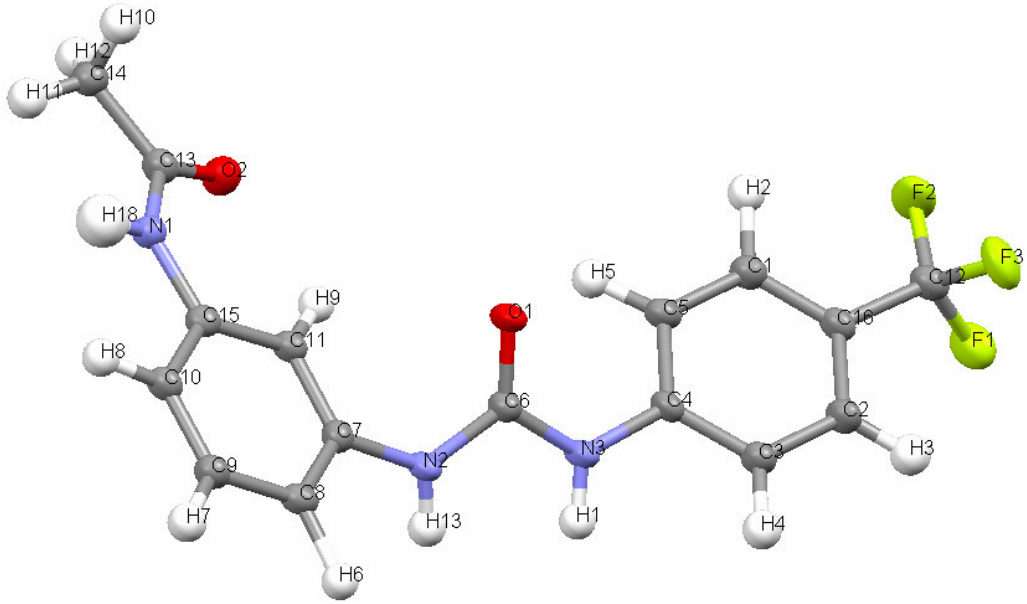

Figure S31. X-ray crystal structure of compound **3** with ellipsoids drawn at the 50% probability level.

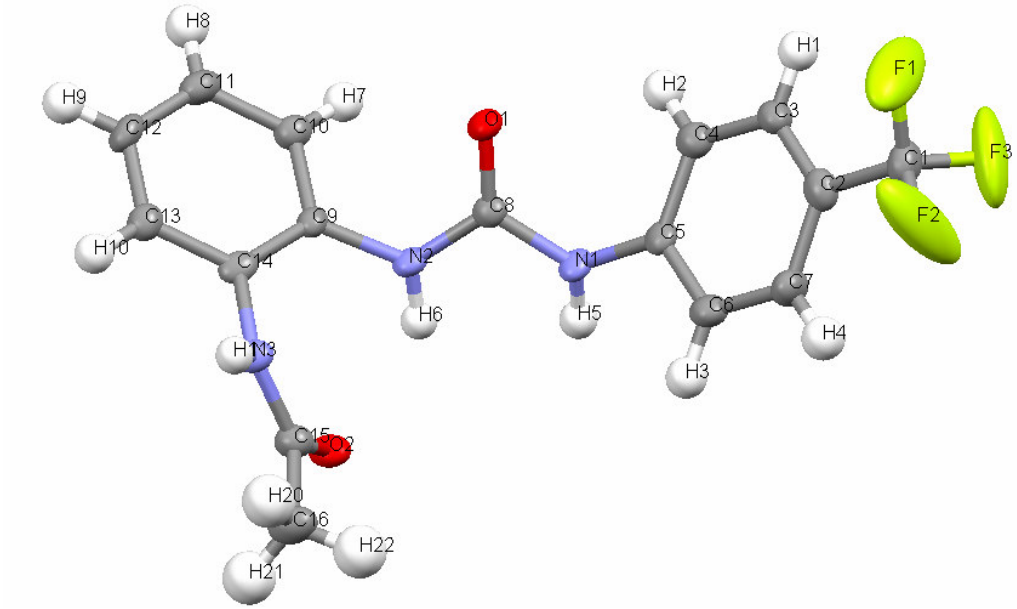

2. Synthesis of intermediates

Procedure 1: General experimental procedure for compounds 7-9

The relevant nitroaniline was placed into a small beaker and acetic anhydride was added. The solution was then stirred at room temperature overnight. The resulting precipitate was then filtered and washed twice with diethyl ether. The solid was collected and dried under vacuum.

Procedure 2: General experimental procedure for compounds 10-12

The relevant nitro acetamide was placed in a 25 mL RBF with the catalyst, 10% Pd/C and CH_3CH_2OH was added. Hydrazine monohydrate was subsequently added and the reaction mixture was stirred at 95˚C overnight under an argon atmosphere. The mixture was filtered while hot, through celite, and the solvent removed under reduced pressure. The obtained solid was washed with diethyl ether. Once collected the solid was dried under vacuum.

N-(4-Nitro-phenyl)-acetamide (7)

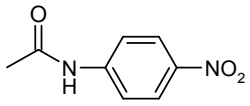

7 was synthesized according to Procedure 1, using 4-nitroaniline (0.7 g, 5.07 mmol). The product was isolated as a pale beige solid (0.76 g, 83% yield). m.p. 208-210 ˚C; ^{1}H NMR (400 MHz, $(CD_3)_2CO$, δ_H) 9.75 (broad s, 1H, NH), 8.22 (d, 2H, CH, J = 9.52 Hz), 7.90 (d, 2H, CH, J = 9.04 Hz), 2.17 (s, 3H, CH_3); ^{13}C NMR (100 MHz, $(CD_3)_2CO$, δ_C) 168.43, 145.03, 142.28, 124.27, 118.06, 117.98, 23.11; IR υ_{max} (cm^{-1}) 3272, 3093, 1680, 1618, 1597, 1565, 1502, 1493, 1403, 1346, 1331, 1302, 1268, 1179, 1113, 1005, 966, 865, 848, 831, 749, 697, 687.

N-(3-Nitro-phenyl)-acetamide (8)

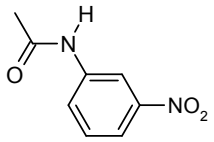

8 was synthesised according to Procedure 1, using 3-nitroaniline (0.68 g, 4.92 mmol). The product was isolated as a pale beige solid (0.50 g, 57% yield). m.p. 148-150 ˚C; ^{1}H NMR (400 MHz, CD_3OD, δ_H) 8.61 (s, 1H, CH), 7.94 (d, 1H, CH, J = 8.04 Hz), 7.85 (d, 1H, CH, J = 7.4 Hz), 7.54 (t, 1H, CH, J = 8.52 Hz, 8.04 Hz), 2.18 (s, 3H, CH_3); ^{13}C NMR (100 MHz, CD_3OD, δ_C) 170.13, 147.99, 139.45, 128.95, 124.39, 117.40, 113.33, 22.04; IR υ_{max} (cm^{-1}) 3289, 3260, 3192, 3129, 3096, 2861, 2809, 1671, 1598, 1547, 1525, 1476, 1424, 1368, 1348, 1324, 1293, 1276, 1260, 1162, 1077, 1016, 983, 885, 822, 804, 759, 737, 690, 669.

N-(2-Nitro-phenyl)-acetamide (9)

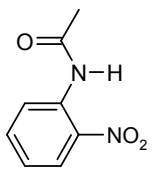

9 was synthesised according to Procedure 1, using 2-nitroaniline (0.51 g, 3.69 mmol). The product was isolated as a bright yellow solid (0.38 g, 57% yield). m.p. 89-91 ˚C; ^{1}H NMR (400 MHz, $CDCl_3$, δ_H) 10.35 (broad s, 1H, NH), 8.78 (d, 1H, CH, J = 8.52 Hz), 8.22 (d, 1H, CH, J = 8.52 Hz), 7.66 (t, 1H, CH, J =

7.28 Hz, 8.52 Hz), 7.20 (t, 1H, CH, *J* = 7.28 Hz, 8.28 Hz), 2.31 (s, 3H, CH_3); ^{13}C NMR (100 MHz, $CDCl_3$, δ_C) 168.62, 135.82, 134.40, 135.54, 125.27, 122.77, 121.71, 25.20; IR υ_{max} (cm^{-1}) 3369, 3090, 1698, 1607, 1583, 1497, 1413, 1367, 1340, 1272, 1225, 1161, 1145, 1083, 1038, 999, 858, 834, 793, 788, 748, 705, 688.

N-(4-Amino-phenyl)-acetamide (10)

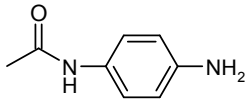

10 was synthesized according to Procedure 2, using N-(4-Nitro-phenyl)-acetamide (**7**) (0.6 g, 3.33 mmol), and hydrazine monohydrate (0.85 g, 26.6 mmol). The product was isolated as an off white solid (0.495 g, 98% yield). m.p. 155-157 ˚C; ^1H NMR (400 MHz, $(CD_3)_2CO$, δ_H) 8.80 (broad s, 1H, NH), 7.33 (d, 2H, CH, *J* = 8.52 Hz), 6.61 (d, 2H, CH, *J* = 9.04 Hz), 4.43 (broad s, 2H, NH_2), 2.00 (s, 3H, CH_3); ^{13}C NMR (100 MHz, $(CD_3)_2CO$, δ_C) 166.58, 143.98, 129.27, 120.26, 113.73, 22.66.

N-(3-Amino-phenyl)-acetamide (11)

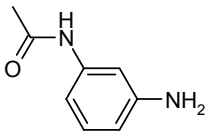

11 was synthesized according to Procedure 2, using N-(3-Nitro-phenyl)-acetamide (**8**) (0.38 g, 2.11 mmol), and hydrazine monohydrate (0.54 g, 17.0 mmol). The product was isolated as a pale pink crystalline solid (0.16 g, 52% yield). m.p. 86-89 ˚C; ^1H NMR (400 MHz, CD_3OD, δ_H) 7.04 (d, 1H, CH, *J* = 8.52 Hz), 7.00 (s, 1H, CH), 6.80 (d, 1H, CH, *J* = 8.00 Hz), 6.48 (d, 1H, CH, *J* = 8.04 Hz), 2.09 (s, 3H, CH_3); ^{13}C NMR (100 MHz, CD_3OD, δ_C) 169.69, 147.42, 138.67, 128.44, 110.77, 109.32, 106.58, 22.00; IR υ_{max} (cm^{-1}) 3376, 3297, 3082, 1671, 1606, 1546, 1491, 1437, 1366, 1323, 1310, 1259, 1188, 1163, 1072, 1014, 966, 988, 847, 773, 687.

N-(2-Amino-phenyl)-acetamide (12)

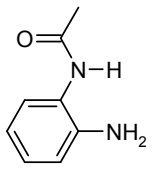

12 was synthesized according to Procedure 2, using N-(2-Nitro-phenyl)-acetamide (**9**) (0.25 g, 1.39 mmol), and hydrazine monohydrate (0.36 g, 11.0 mmol). The product was isolated as an off white crystalline solid (0.21 g, 99% yield). m.p. 126-128 ˚C; ^1H NMR (400 MHz, CD_3OD, δ_H) 7.09 (d, 1H, CH, *J* = 7.52 Hz), 7.03 (t, 1H, CH, *J* = 7.52 Hz), 6.85 (d, 1H, CH, *J* = 7.52 Hz), 6.72 (t, 1H, CH, *J* = 7.52 Hz), 2.16 (s, 3H, CH_3); ^{13}C NMR (100 MHz, CD_3OD, δ_C) 170.39, 141.50, 126.45, 125.34, 123.16, 117.56, 116.58, 21.12; IR υ_{max} (cm^{-1}) 3455, 3363, 3271, 3046, 2927, 1638, 1586, 1533, 1496, 1456, 1369, 1299, 1255, 1219, 1156, 1138, 1042, 1012, 963, 924, 858, 847, 742.